A three dimensional hydrogen bonded organic framework assembled through antielectrostatic hydrogen bonds

Duncan A. Cullen, Michael G. Gardiner and Nicholas G. White*

Research School of Chemistry, The Australian National University, Canberra, ACT, Australia

Email: nicholas.white@anu.edu.au

URL: www.nwhitegroup.com

Synthesis and characterization

General remarks

The tetraamidinium compound **1·Cl$_4$** was prepared as previously described.[S1] All other compounds, including solvents, were bought from commercial suppliers and used as received.

NMR spectra were collected on a Bruker Avance 400 spectrometer and are referenced to the residual solvent signal.[S2] High resolution electrospray ionisation mass spectra (HRESI-MS) were recorded on a Waters LCT Premier instrument. Infrared spectra were recorded on a Perkin-Elmer Spectrum Two FT-IR Spectrometer fitted with an ATR Two Single Reflection Diamond. Elemental analysis data were collected at London Metropolitan University using a Thermoscientific Flash 2000 Elemental Analyser. Thermogravimetric analysis data were recorded on a TA Instruments Q500 analyser under flowing nitrogen gas. PXRD data were recorded at room temperature on a PANalytical Empyrean diffractometer using Cu Kα radiation and a PIXcel detector.

Synthesis of 1·(HCO$_3$)$_4$

The tetraamidinium **1·Cl$_4$** (0.063 g, 0.10 mmol) was dissolved in H_2O (20 mL), and $NaHCO_3$ (0.42 g, 5.0 mmol) was dissolved in H_2O (20 mL). The two solutions were mixed to give a clear colourless solution. This was left to stand, resulting in the formation of crystals within 2 days. After 10 days, the crystals were isolated by filtration, washed with water (5 × 5 mL) and air-dried to give the framework as white crystals. Yield: 0.049 g (0.063 mmol, 63%)*.

^{1}H NMR [d$_6$-DMSO containing a drop of 20% DCl in D_2O]: 9.58 (br. s, 8H†), 9.30 (br. s, 8H†), 7.92 (d, *J* = 8.6 Hz, 8H), 7.52 (d, *J* = 8.6 Hz, 8H) ppm. ATR-IR (*inter alia*): 1698, 1669, 1400, 1378, 1305 cm^{-1} (C=O, C–O stretches). EA: C 50.7, H 5.1, N 14.1; calc. for [**1·(HCO$_3$)$_4$**]·2.5H_2O ($C_{33}H_{41}N_8O_{14.5}$): C 50.7, H 5.3, N 14.3%.

** Mmol and % yield account for presence of 2.5 molecules of water per framework, as indicated by elemental and thermogravimetric analyses.*
† Due to H/D exchange, these protons integrate to a value less than the expected 8H.

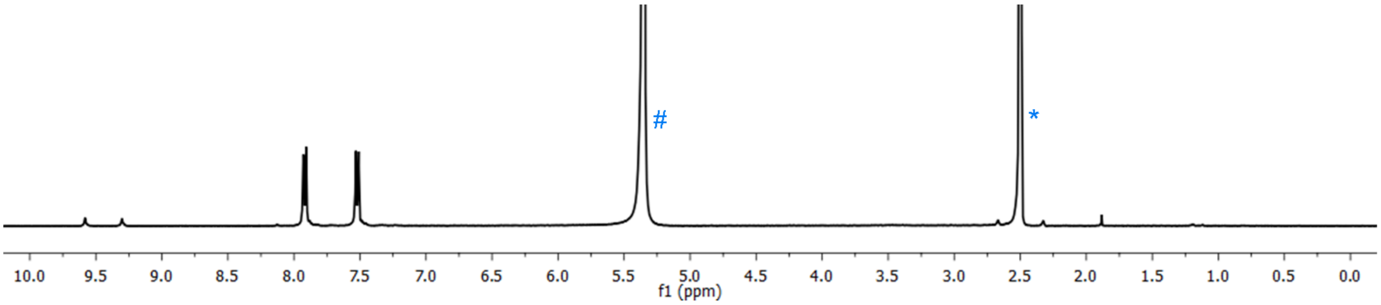

Figure S1. ^{1}H NMR spectrum of [**1·(HCO$_3$)$_4$**], * indicates residual NMR solvent signal, # indicates water [400 MHz, 298 K, d$_6$-DMSO containing a drop of 20% DCl in D_2O].

Powder X-ray diffraction data for **1·(HCO$_3$)$_4$**

The PXRD trace for bulk air-dried **1·(HCO$_3$)$_4$** is shown in Figure S2. The bulk PXRD data are generally consistent with the SCXRD structure. We attribute small differences in the measured and calculated patterns to the differences in temperature at which the PXRD data (293 K) and SCXRD data (150 K) were recorded as well as possible minor changes in unit cell parameters induced by drying the framework.

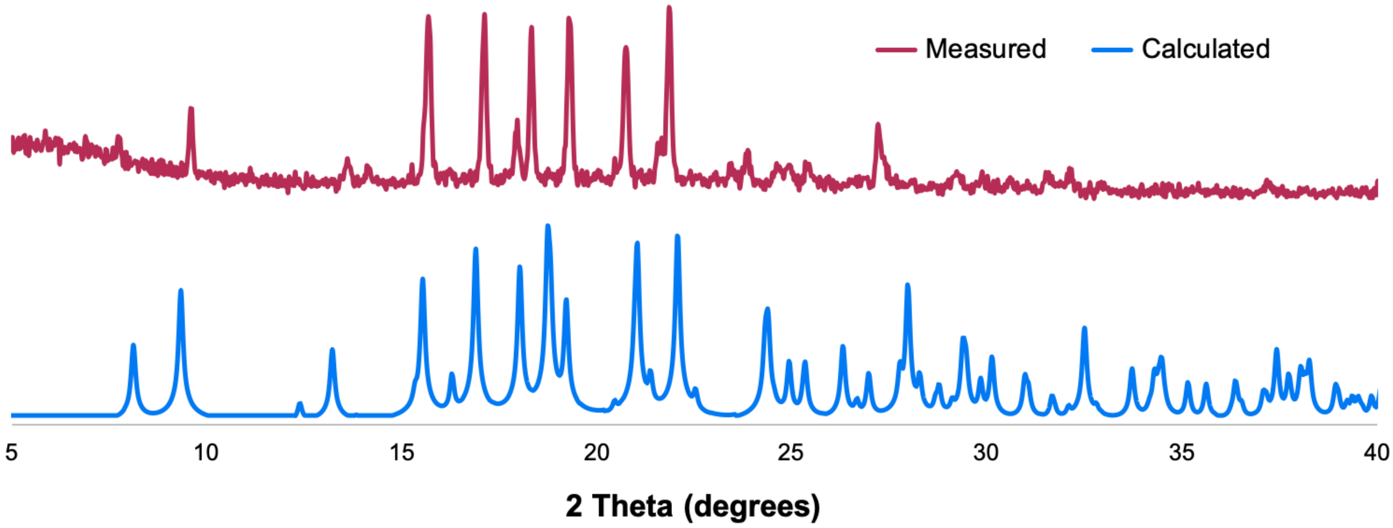

Figure S2. PXRD trace of **1·(HCO$_3$)$_4$** (top, maroon) and comparison with PXRD pattern calculated from SCXRD data (bottom, blue).

Thermogravimetric analysis of **1·(HCO$_3$)$_4$**

The TGA trace of bulk air-dried **1·(HCO$_3$)$_4$** is shown in Figure S3. This trace was collected at 5 °C/minute. The low temperature (< 300 °C) region of the trace was then re-collected at 1 °C/minute (Figure S4). Initial heating causes a small loss of mass consistent with the loss of the 2.5 molecules of water indicated by elemental analyses (2.5 water molecules = 5.8% mass loss). Subsequent heating results in a major loss consistent with the loss of four water molecules and four molecules of carbon dioxide (*i.e.* conversion of the tetraamidinium bicarbonate salt to the tetraamidine, **2**). At higher temperatures, a mass loss corresponding to four molecules of ammonia (*i.e.* conversion to the tetranitrile, **3**) is observed. Tetraamidine **2** was prepared and fully characterised by heating a sample of **1·(HCO$_3$)$_4$** (see next section), while further evidence for decomposition to tetranitrile **3** was provided by ^{1}H NMR spectroscopy (comparison with a sample of pure **3**) and IR spectroscopy (C≡N stretch at 2227 cm^{-1}).

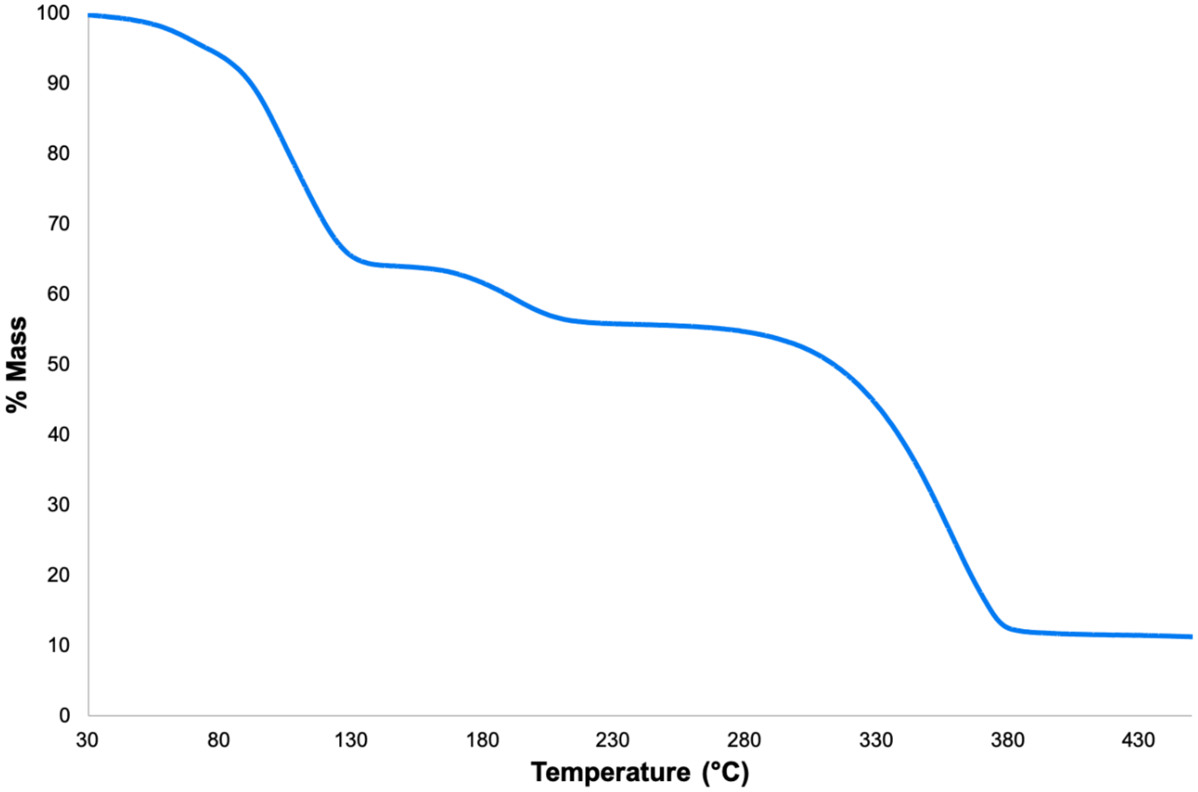

Figure S3. TGA trace of **1·(HCO$_3$)$_4$** (heating rate: 5 °C/min).

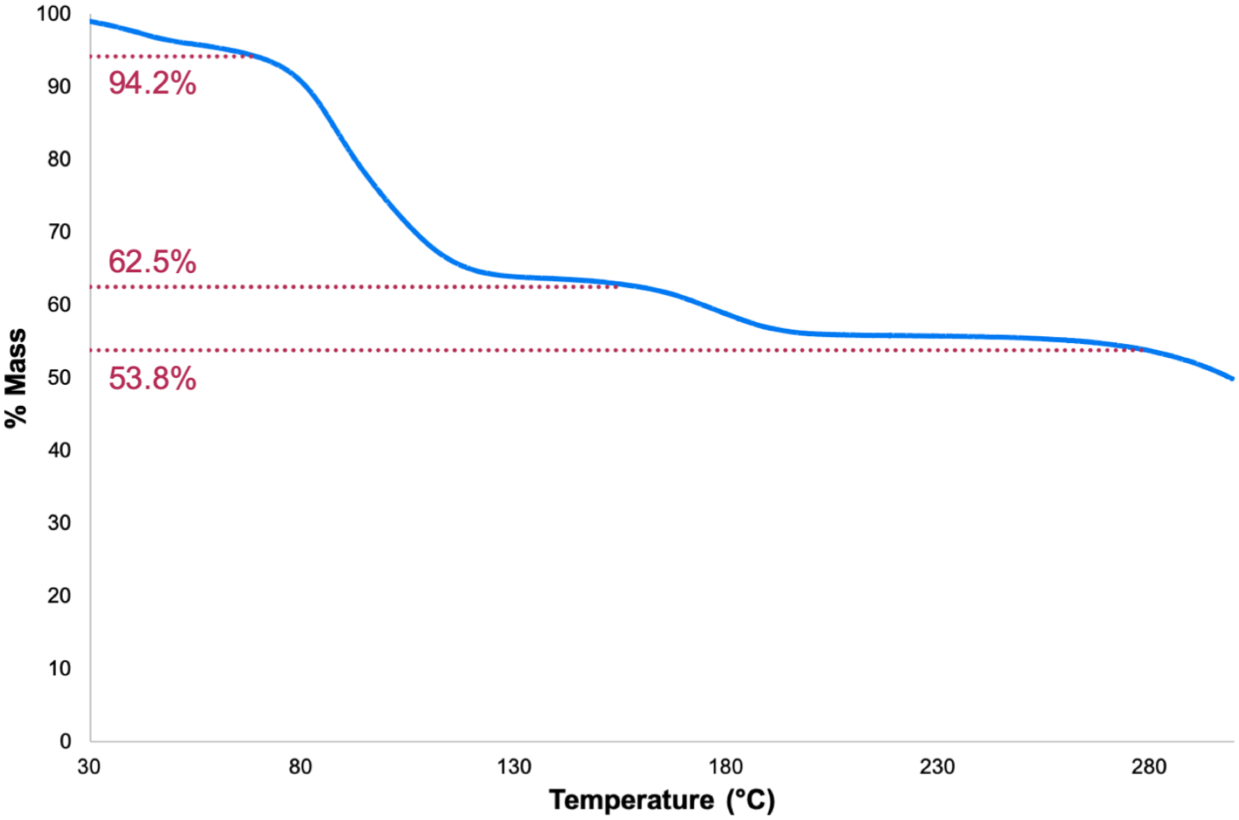

Figure S4. TGA trace of **1·(HCO$_3$)$_4$** (heating rate: 1 °C/min); masses of 94.2% corresponding to the anhydrous framework, 62.5% corresponding to tetraamidine **2**, and 53.8% corresponding to tetranitrile **3** are marked.

Synthesis of 2

A solid sample of crystalline **1·(HCO$_3$)$_4$**·2.5H$_2$O (10 mg, 0.013 mmol) was placed in a small glass sample vial. This was placed in an oil-bath held at 95 °C for 2 hours to give **2** as a slightly off-white microcrystalline solid. Yield: 6.5 mg (0.013 mmol, 100%).

During heating there was no clear visible change in the material, but a significant loss of mass was observed. The product appears visibly crystalline but is amorphous according to PXRD.

^{1}H NMR (d$_6$-DMSO): 7.70 (d, *J* = 8.0 Hz, 8H), 7.24 (d, *J* = 8.0 Hz, 8H), 6.46 (br. s, 12H) ppm. ^{13}C NMR (d$_6$-DMSO): 162.3, 147.5, 134.1, 129.9, 126.3, 64.2 ppm. HRESI-MS (pos.): 489.2513, calc. for **2**: $[C_{29}H_{28}N_8 \cdot H]^+$ = 489.2515 Da. ATR-IR (*inter alia*): 1594, 1482, 1386, 1337 cm^{-1}.

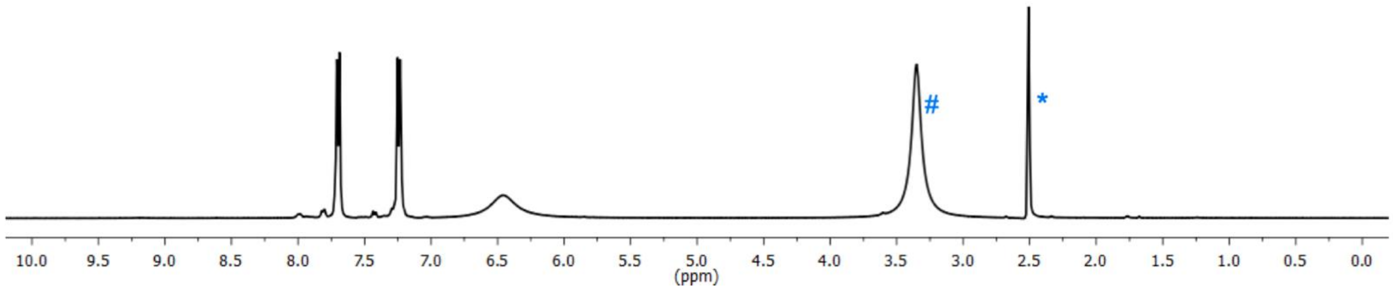

Figure S5. ^{1}H NMR spectrum of **2** prepared by heating a solid sample of **1·(HCO$_3$)$_4$**, * indicates residual NMR solvent signal, # indicates water [400 MHz, 298 K, d$_6$-DMSO].

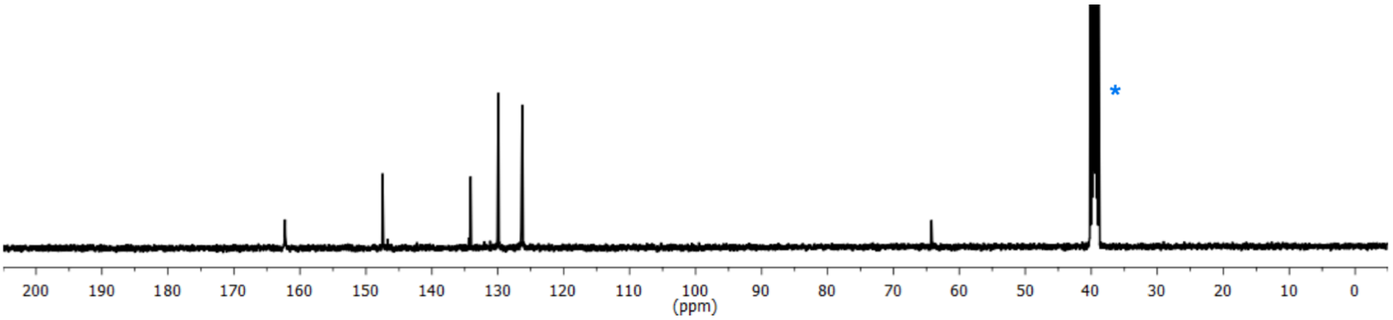

Figure S6. ^{13}C NMR spectrum of prepared by heating a solid sample of **1·(HCO$_3$)$_4$**, * indicates residual NMR solvent signal [101 MHz, 298 K, d$_6$-DMSO].

Solid state conversion of 1·(HCO$_3$)$_4$ to 2: The solid state conversion of **1·(HCO$_3$)$_4$** to **2** does not appear to be particularly sensitive to temperature or time with very similar conversion and purity obtained with heating at 95, 100 or 110 °C and for reaction times of 1 or 2 hours. A small trace (~ 5%) of tetranitrile **3** is always observed as an impurity. Interestingly, using significantly higher temperatures does not appear to have a dramatic effect, *e.g.* heating for 1 hour at 160 °C still gives **2**, although the ratio of **2**:**3** is approximately 85:15 instead of ~ 95:5 when prepared at 95 °C.

Solution conversion of 1·(HCO$_3$)$_4$ to 2: It was also possible to prepare **2** by heating **1·(HCO$_3$)$_4$** in DMSO. Solid **1·(HCO$_3$)$_4$**·2.5H$_2$O (4.7 mg, 6.0 μmol) was suspended in d$_6$-DMSO (0.60 mL, *i.e.* a 10 mM suspension). The suspension was heated to 50 °C over the weekend (~ 64 hours), during which time the suspension cleared to give a colourless solution. The solution was then cooled to room temperature (all material remained in solution when cooled), 1,4-dioxane was added as an internal standard to measure conversion, and the solution analysed by ^{1}H NMR spectroscopy (Figure S7). This showed complete conversion to tetraamidine **2**, with purity slightly better than the sample prepared by solventless heating (Figure S5). Very small traces of tetranitrile **3** were visible in the ^{1}H NMR spectrum.

1·(HCO$_3$)$_4$ could also be converted to **2** by heating at 100 °C for 1 hour in d$_6$-DMSO. This gave complete conversion and product of essentially identical purity to that shown in Figure S7.

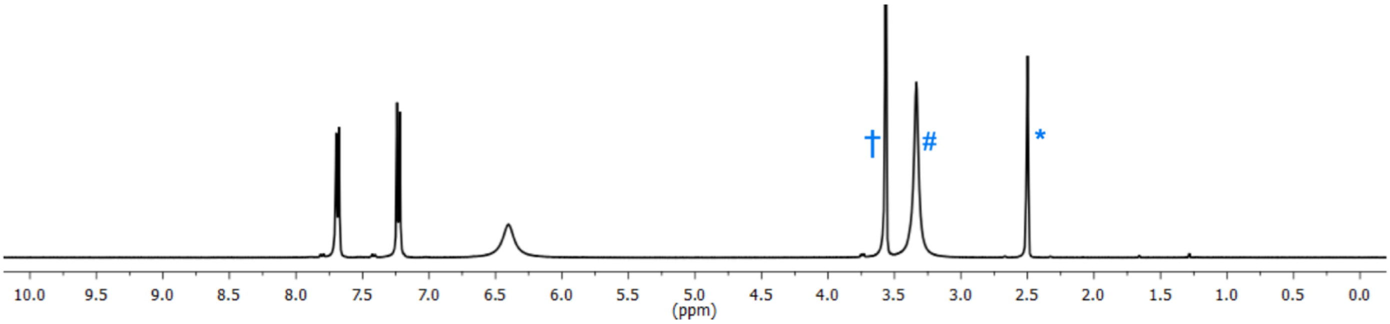

Figure S7. ^{1}H NMR spectrum of **2** prepared by heating **1·(HCO$_3$)$_4$** in d$_6$-DMSO; * indicates residual NMR solvent signal, # indicates water, † corresponds to 1,4-dioxane used as an internal standard [400 MHz, 298 K, d$_6$-DMSO].

X-ray crystallography

Data collection and refinement

General Comments: Full crystallographic data in CIF formatted have been uploaded to the Cambridge Structural Database (CCDC Numbers: 1949478 and 1949479). Thermal ellipsoid plots are provided in Figures S8 and S9; selected crystallographic data are summarized in Table S1.

$1\cdot(HCO_3)_4\cdot 3H_2O$: Data were collected using mirror-monochromated Cu Kα radiation on an Agilent SuperNova diffractometer. Crystals were cooled to 150 K using a Cryostream N2 open-flow cooling device.[S3] Raw frame data (including data reduction, interframe scaling, unit cell refinement and absorption corrections) were processed using CrysAlisPro.[S4] SHELXT[S5] and SHELXL[S6] were used for structure solution and refinement within OLEX2.[S7]

Solution and refinement in the non-ambiguous space group $P4_2/nbc$ clearly revealed a number of independent occupancy disorders in all components of the structure. The refinement model was validated as not relating to space group assignment issues by solution and refinement in $P1$ that also showed all the non-hydrogen atom occupancy disorders as described below. Where not implied by the non-hydrogen atom occupancies or site symmetry, the model for hydrogen atom disordering in $P4_2/nbc$ was guided by difference maps.

The unique arene ring of the tetraarylmethane cationic unit in the asymmetric unit displayed two ring conformations that were refined as complementary occupancies of 0.792:0.208 and later fixed at these occupancies. The major/minor occupancies of the four arene ring orientations within each cationic unit are linked in order to avoid steric interactions with adjacent rings within the cation but these occupancies do not appear to influence the anion/solvent regions of the structure based on the occupancy ratios described below for the other disorders in the structure. The amidinium substituents of the tetraarylmethane cations were not disordered and H-bond with both chemically inequivalent bicarbonate anion pairs in the structure as well as water molecules.

Disorder in the bicarbonate dimers that H-bond to the amidinium units through pairs of N–H···O H-bonds [*i.e.* O(11), O(12) and C(11)] appears limited to the hydrogen atoms of the bicarbonate units and is crystallographically required from the C_2 axis passing through the anion. The other bicarbonate dimers [located in the pores of the framework, *i.e.* O(21), O(22), O(23) and C(21)] are associated with the amidinium units by single N–H···O H-bonds and lie on higher symmetry sites. They are severely disordered, with the site symmetry implying equal occupancies for two positions of the anions, with the hydrogen atom location featuring some disorder. The C-O distances in this bicarbonate anion were restrained at estimated distances with DFIX cards.

There are three water molecules that are also disordered, with their strict 50% occupancies across symmetry related sites appearing to be complementary to the disordered occupancies of the disordered bicarbonate pairs described above. The location of the oxygen atoms of the water molecules is consistent with chains of three H-bonded water molecules that also H-bond to the disordered bicarbonate pairs and the amidinium units. Given the partial occupancy of these water molecules and their disordered nature, it was not possible to identify the position of their H-atoms. The solvent inclusion model was consistent with microanalytical and thermogravimetric analysis data.

$2\cdot4CH_3OH$: Data were collected using mirror-monochromated Cu Kα radiation on an Agilent SuperNova diffractometer. Crystals were cooled to 150 K using a Cryostream N2 open-flow cooling device.[S3] Raw frame data (including data reduction, interframe scaling, unit cell refinement and absorption corrections) were processed using CrysAlisPro.[S4] The structure was solved with SUPERFLIP[S8] and refined using full-matrix least-squares on F^2 within the CRYSTALS suite.[S9] C–H hydrogen atoms were visible in the Fourier difference map, and were initially refined with restraints on bond lengths and angles after which the positions were used as the basis for a riding model.[S10] O–H and N–H hydrogen atoms were visible in the Fourier difference map, and their positions were refined with restraints on bond lengths and angles.

Thermal ellipsoid plots

$1\cdot(HCO_3)_4\cdot3H_2O$:

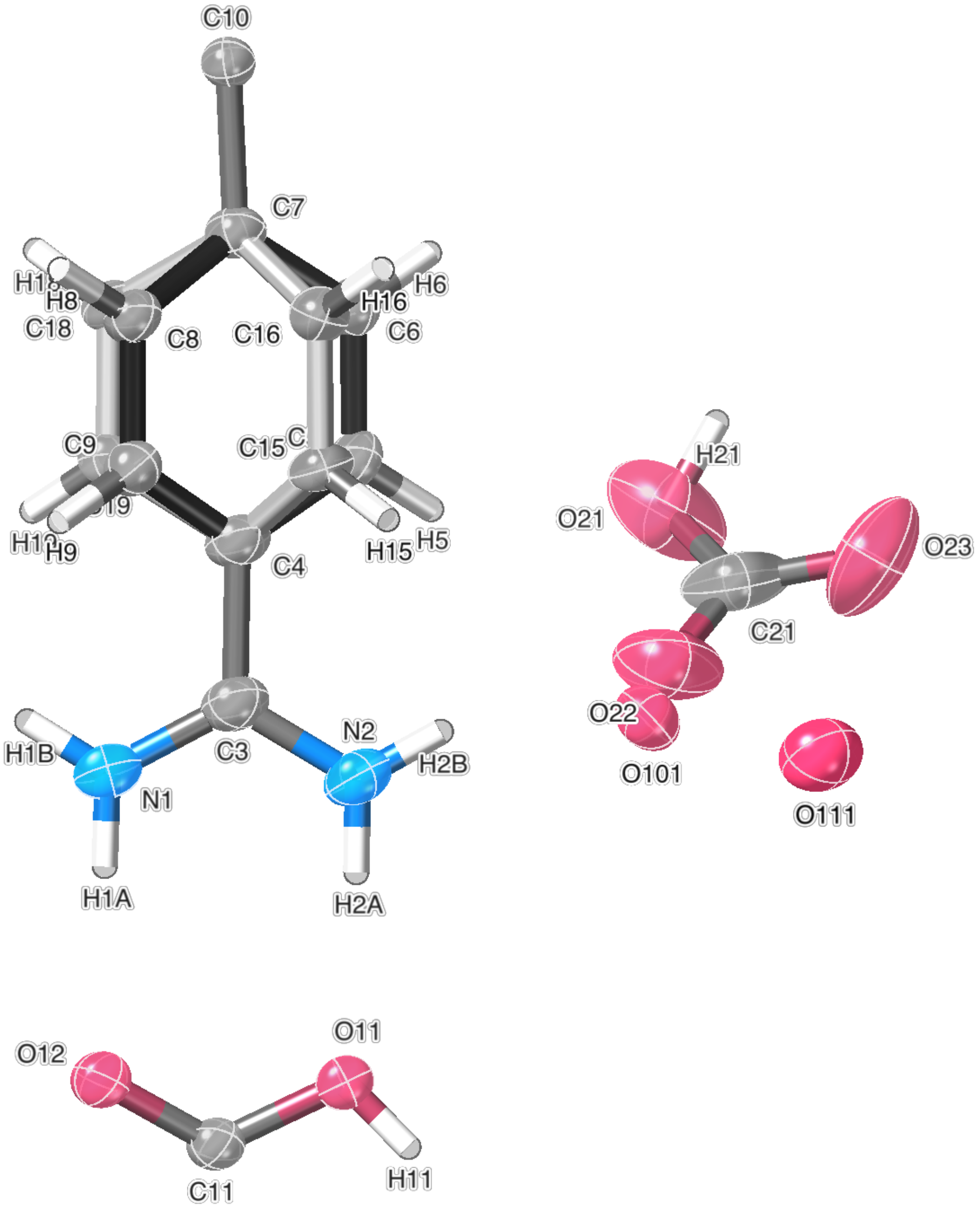

Figure S8. Thermal ellipsoid plot showing asymmetric unit of **$1\cdot(HCO_3)_4$**$\cdot3H_2O$. Ellipsoids are shown at 50% probability level. Both positions of the phenyl ring disorder (occupancies: 0.792:0.208) are shown. One of the bicarbonate anions (C21–O23), and both water molecules are half occupancy and are disordered over a special position (see structure description); it was not possible to locate the hydrogen atoms on the half occupancy water molecules.

2·4CH$_3$OH:

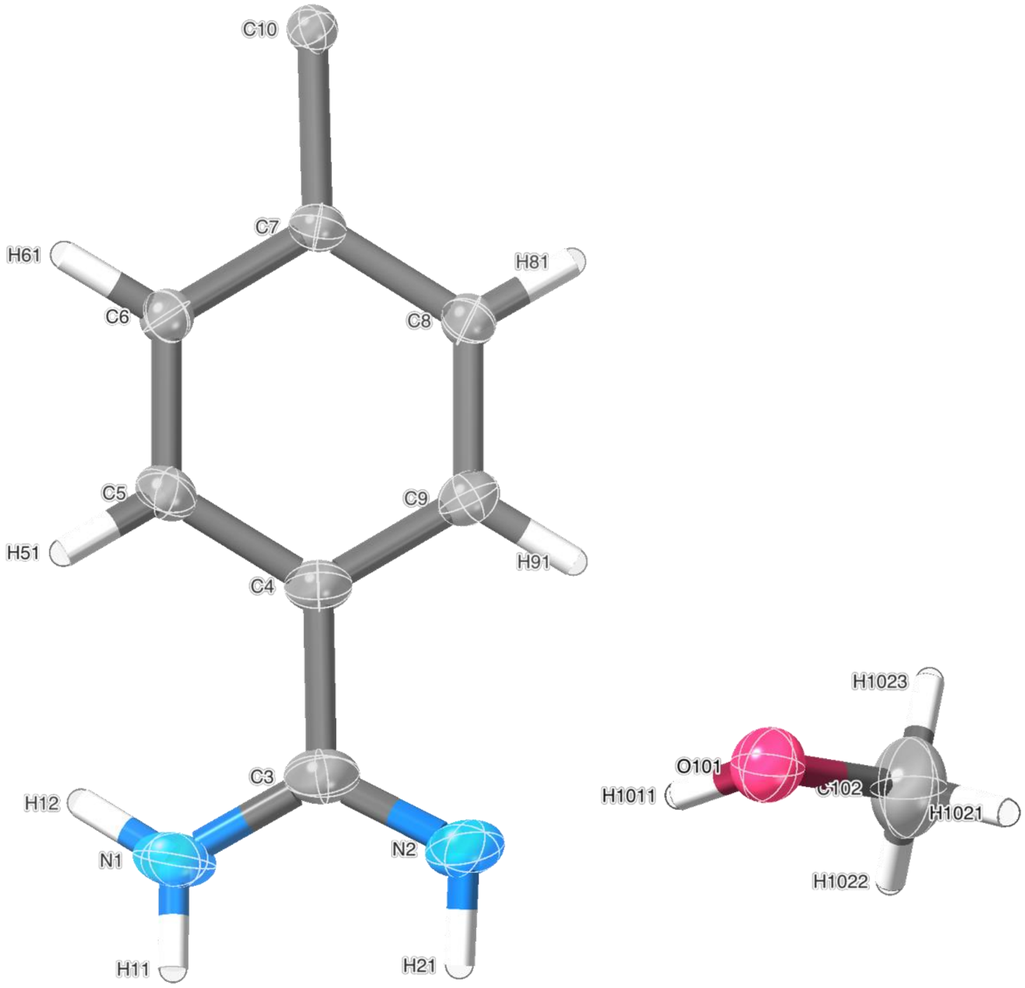

Figure S9. Thermal ellipsoid plot showing asymmetric unit of **2**·4CH$_3$OH. Ellipsoids are shown at 50% probability level.

Additional views of structures

1·$(HCO_3)_4$·$3H_2O$:

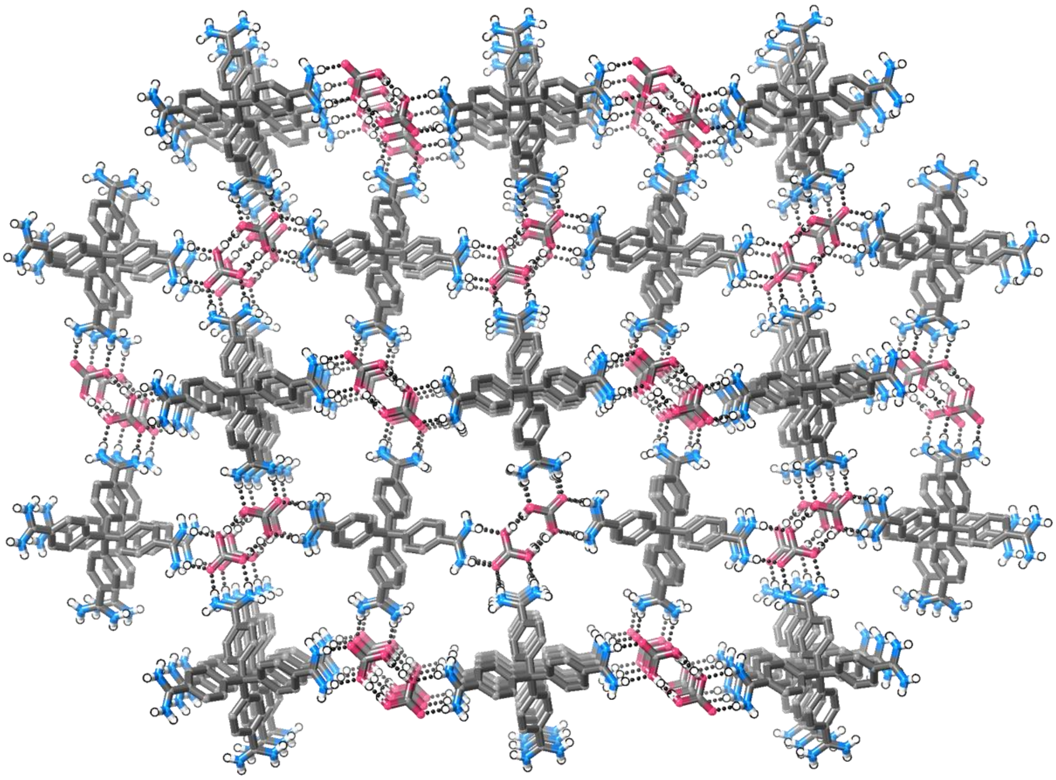

Figure S10. View of a single net of **1·$(HCO_3)_4$**·$3H_2O$. C–H hydrogen atoms, water molecules, and bicarbonate dimers in the pores of the networks are omitted for clarity.

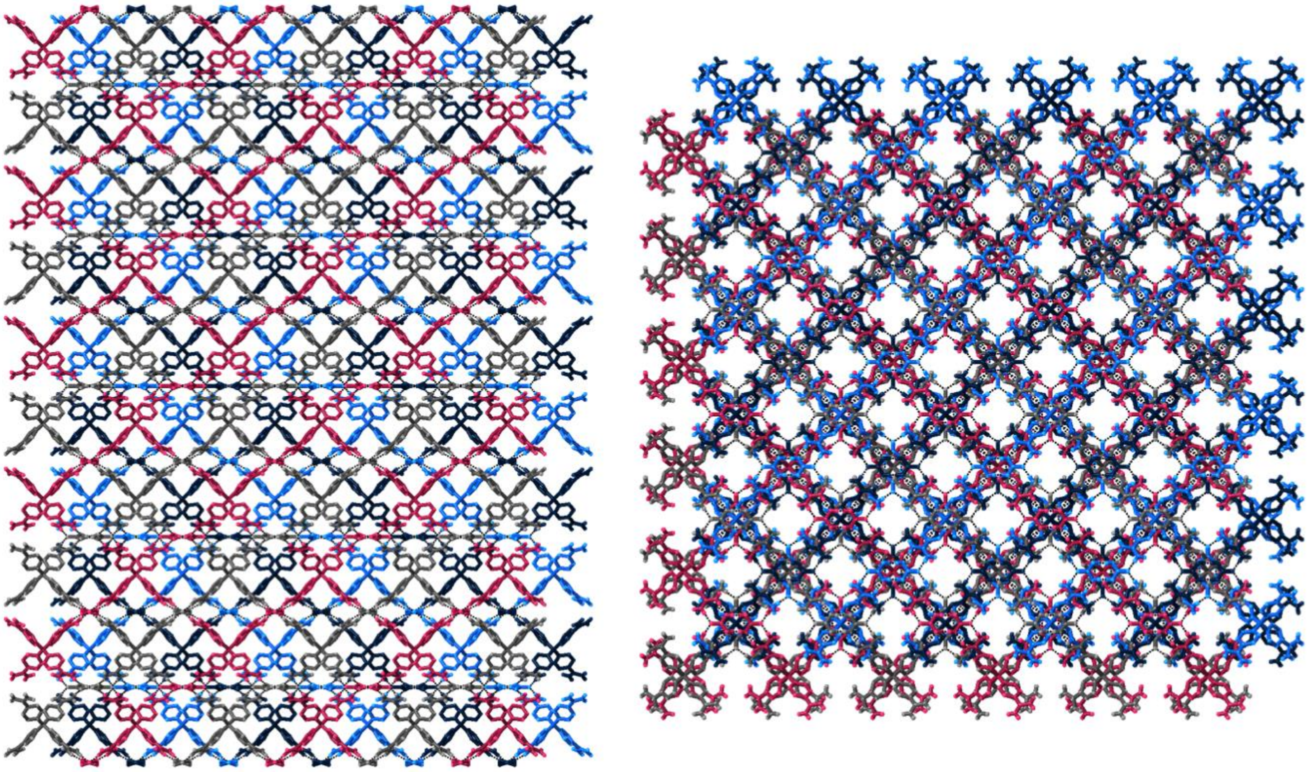

Figure S11. Two different views of the four interpenetrating H-bonded diamondoid nets in the structure of **1·$(HCO_3)_4$**·$3H_2O$, each net is shown in a different colour. C–H hydrogen atoms, water molecules, and bicarbonate dimers in the pores of the networks are omitted for clarity.

2·4CH$_3$OH:

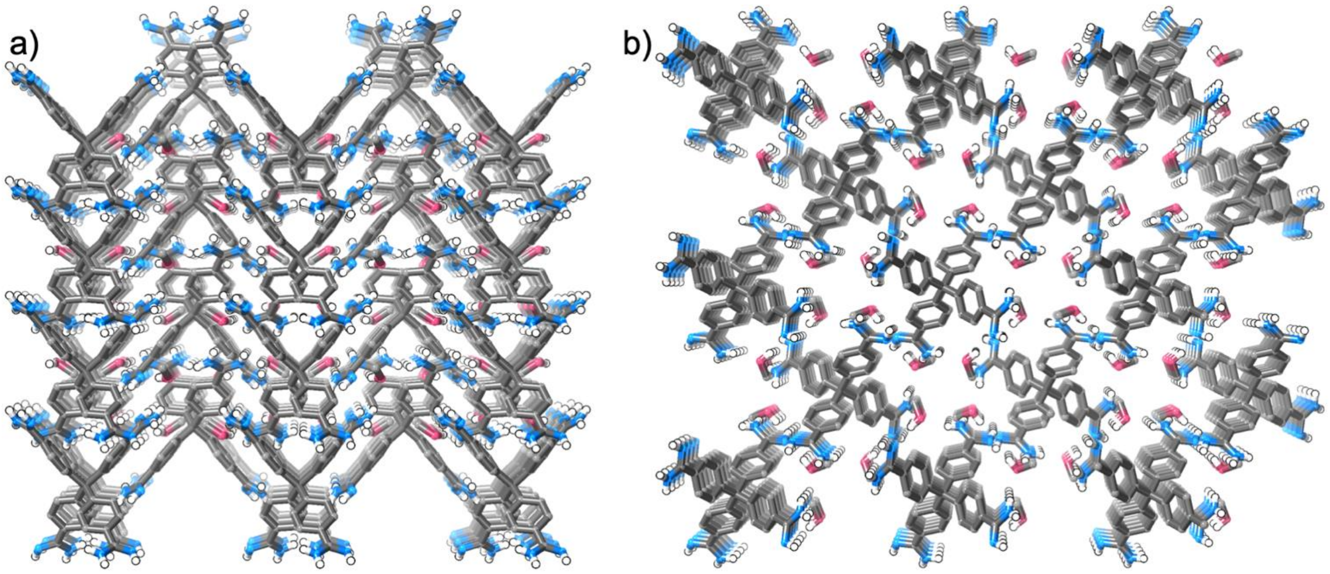

Figure S12. Packing diagram for **2**·4CH$_3$OH, viewed down a) the *a*-axis; and b) the *c*-axis. C–H hydrogen atoms are omitted for clarity.

Table of crystallographic data

Table S1. Selected crystallographic data.

Compound	**1·(HCO$_3$)$_4$**·3H$_2$O	**2**·4CH$_3$OH
Radiation type	Cu (λ = 1.54184 Å)	Cu (λ = 1.54184 Å)
Formula	$C_{29}H_{32}N_8\cdot(HCO_3)_4\cdot3O^a$	$C_{29}H_{28}N_8\cdot4(CH_4O)$
Formula weight	784.70	616.76
a (Å)	13.38177(8)	14.533300(16)
b (Å)	13.38177(8)	14.533300(16)
c (Å)	21.75010(18)	7.836020(13)
α (º)	90	90
β (º)	90	90
γ (º)	90	90
Unit cell volume (Å^3)	3894.83(6)	1655.099(5)
Crystal system	tetragonal	tetragonal
Space group	*P*4$_2$/*nbc*	*P*4$_2$/*n*
Z	4	2
Reflections (all)	24851	8618
Reflections (unique)	1976	1665
R_{int}	0.023	0.031
R_1 [$I > 2\sigma(I)$]	0.081	0.050
$wR_2(F^2)$ (all data)	0.247	0.135
CCDC number	1949479	1949478

[a] It was not possible to locate the hydrogen atoms on the partial occupancy water molecules.

References

[S1] M. Morshedi, M. Thomas, A. Tarzia, C. J. Doonan, N. G. White, Supramolecular anion recognition in water: synthesis of hydrogen-bonded supramolecular frameworks, *Chem. Sci.* **2017**, *8*, 3019–3025.

[S2] H. E. Gottlieb, V. Kotlyar, A. Nudelman, NMR chemical shifts of common laboratory solvents as trace impurities, *J. Org. Chem.* **1997**, *62*, 7512–7515.

[S3] J. Cosier, A. M. Glazer, A nitrogen-gas-stream cryostat for general X-ray diffraction studies, *J. Appl. Crystallogr.* **1986**, *19*, 105–107.

[S4] Agilent Technologies, *CrysAlisPro*, **2011**.

[S5] G. M. Sheldrick, *SHELXT* – Integrated spage-group and crystal-structure determination, *Acta Crystallogr.* **2015**, *A71*, 3–8.

[S6] G. M. Sheldrick, Crystal structure refinement with *SHELXL*, *Acta Crystallogr.* **2015**, *C71*, 3–8.

[S7] O. V. Dolomanov, L. J. Bourhis, R. J. Gildea, J. A. K. Howard, H. Puschmann, *OLEX2:* a complete structure solution, refinement and analysis program, *J. Appl. Crystallogr.* **2009**, *42*, 335–341.

[S8] L. Palatinus, G. Chapuis, SUPERFLIP. A computer program for the solution of crystal structures by charge flipping in arbitrary dimensions, *J. Appl. Crystallogr.* **2007**, *40*, 786–790.

[S9] P. W. Betteridge, J. R. Carruthers, R. I. Cooper, K. Prout, D. J. Watkin, CRYSTALS version 12: software for guided crystal structure analysis, *J. Appl. Crystallogr.* **2003**, *36*, 1487.

[S10] R. I. Cooper, A. L. Thompson, D. J. Watkin, CRYSTALS enhancements: dealing with hydrogen atoms in refinement, *J. Appl. Crystallogr.* **2010**, *43*, 1100–1107.